Water-Absorption Kinetics and Water-State Dynamics of Astragalus Membranaceus from Different Origins Probed by Low-Field NMR Transverse Relaxation

Huiren Xu[1,#], Cheng Ni[1,2,#], Wei He[3], Fang Yang[1,*], Dingguo Li[4], Limin He[1,5,*]
[1]School of Intelligent Medicine and Technology, Hainan Medical University, Haikou, China
[2]School of Clinical Medicine, Hainan Medical University, Haikou, China
[3]The Second Clinical Medical College of Hainan Medical University, Haikou, China
[4]School of Basic Medical Sciences, Hainan Medical University, Haikou, China
[5]Key Laboratory of Tropical Translational Medicine of Ministry of Education, School of Public Health, Hainan Academy of Medical Sciences, Hainan Medical University, Haikou, China
**Corresponding Author*
#Huiren Xu and Cheng Ni contributed equally to this work

Abstract: The quality of Astragalus membranaceus crude drug is closely associated with the tissue microstructure inherited from the cultivation environment. In this study, the water-absorption behaviours of A. membranaceus harvested from four cultivation regions (Gansu, Inner Mongolia, Shanxi and Yunnan) were examined by low-field nuclear magnetic resonance (LF-NMR) transverse-relaxation measurements combined with gravimetric monitoring. Distinct water-uptake profiles were observed across provenances: Shanxi samples absorbed water most rapidly (48.8 % at 5 min and above 70 % at 15 min), whereas Gansu samples absorbed water most slowly (17.3 % at 30 min, approaching 70 % only after 360 min). The mass-time trajectories of the Gansu, Shanxi and Inner-Mongolia batches were well described by a two-phase exponential decay function with coefficients of determination exceeding 0.999, while the Yunnan batch required a two-phase exponential association function. T2 inversion spectra resolved three water populations, i.e. tightly bound water (T21, 0.01–1 ms), semi-bound water (T22, 1–10 ms) and free water (T23, 10–100 ms), whose signal amplitudes rose continuously and shifted rightward during immersion. A strong positive linear correlation ($R^2 > 0.99$) was established between total sample mass and total NMR peak area for all four origins. These results show that LF-NMR transverse-relaxation signals offer a rapid, non-destructive and microstructure-sensitive probe of water-absorption kinetics in medicinal herbs, providing a physical basis for subsequent quality and origin evaluation of porous herbal matrices.

Keywords: Astragalus Membranaceus; Low-Field Nuclear Magnetic Resonance; Transverse Relaxation; Water-Absorption Kinetics, Water State; Carr-Purcell-Meiboom-Gill Sequence

1. Introduction

Traditional Chinese medicine (TCM) has accumulated thousands of years of clinical practice, and the quality of medicinal materials is widely regarded as the foundation for the sustainable development of the TCM industry [1,2]. Among the several hundred frequently used herbs, Astragalus membranaceus stands out for its broad applications in immune regulation and chronic-disease management; flavonoids, polysaccharides and saponins are the major bioactive fractions underlying these effects [3]. Because the herb is cultivated over large geographic areas, the intrinsic quality of commercial batches varies considerably, and consumers and regulators increasingly demand objective criteria that reflect the authenticity of the raw material [1].

Conventional quality assessment of Astragalus membranaceus relies mainly on quantifying characteristic chemical constituents, which usually requires tedious sample preparation, dedicated chromatographic or spectroscopic instruments and lengthy analytical runs [3]. By contrast, low-field nuclear magnetic resonance (LF-NMR) is a non-destructive technique that probes hydrogen protons in water and organic

 Copyright @ STEMM Institute Press

matter directly, without chemical pre-treatment, and responds rapidly to changes in proton abundance and molecular mobility [4,5]. Time-domain NMR relaxometry and imaging have been applied to food quality evaluation [4], edible-oil authentication [5], compositional analysis of oils and lipids [6,7], frying-oil monitoring [8], moisture dynamics in maize kernels [9] and oil-content determination in soybeans [10], underscoring the utility of proton-relaxation measurements for hygroscopic, porous biological matrices.

Dried herbal roots are porous materials in which the internal structure governs water penetration and retention; their water-absorption behaviour may therefore carry microstructural fingerprints of geographical origin. In this work, the CPMG pulse sequence was used to record transverse-relaxation signals of A. membranaceus samples from four producing regions throughout the water-absorption process. The aims were threefold: (i) to quantify origin-dependent water-uptake rates and establish mass-time fitting functions; (ii) to characterise the evolution of bound and free water fractions from T2 inversion spectra; and (iii) to verify the linear correspondence between gravimetric mass gain and NMR signal intensity, thereby validating LF-NMR as a reliable proxy for monitoring water-absorption dynamics.

2. Materials and Methods

2.1 Materials

Dried root samples of Astragalus membranaceus were collected from four representative cultivation areas: Longxi (Gansu Province), Chifeng (Inner Mongolia Autonomous Region), Datong (Shanxi Province) and Dali (Yunnan Province). All materials were air-dried under natural conditions and stored in sealed containers before measurement.

2.2 Instruments

A low-field NMR analyser (MesoMR23-060H-I, Suzhou Niumag Electronic Technology Co., Ltd., China) equipped with a permanent magnet of 0.5 T field strength, a 60-mm-diameter probe coil and a magnet temperature of 32 °C was used for all relaxation measurements. An electronic balance (FS-1004, Shanghai Shangtian Precision Instrument Co., Ltd., China) was employed for gravimetric determination, and weighing bottles were supplied by Suqian Gudi E-commerce Co., Ltd., China.

2.3 Water-Absorption Rate Measurement

For each origin, three groups of dried samples with similar initial masses were prepared for parallel experiments, and the immersion time at which the sample mass no longer changed was defined as the saturation point. The saturation times of the Gansu, Shanxi, Inner-Mongolia and Yunnan batches were 480, 60, 60 and 120 min, respectively. Sampling intervals were arranged according to the saturation characteristics of each origin. The water-absorption rate was calculated as $[(Mt - M0)/M0] \times 100\ \%$, where Mt is the average mass at a given immersion time and M0 is the initial mass.

2.4 Water-State Characterisation by CPMG Measurement

Samples from each origin were positioned at the centre of the permanent magnetic field, and a hard-pulse free induction decay (FID) sequence was first used to determine the centre frequency. The Carr-Purcell-Meiboom-Gill (CPMG) sequence was then applied to acquire the transverse-relaxation time T2 of the samples. After the samples reached saturation, they were removed from the water bath, blotted with filter paper to remove surface water and re-positioned at the centre of the magnetic field for a second CPMG measurement. All T2 inversion data were processed with the Niumag magnetic-resonance signal analysis software.

2.5 Function Fitting

The relationship between total average mass and total average peak area was fitted with Origin 2022 software (OriginLab Corporation, USA). Non-linear regression was performed with the Levenberg-Marquardt algorithm, and the coefficient of determination (R^2) was used to evaluate the goodness of fit.

3. Results and Discussion

3.1 Water-Absorption Rate of Astragalus from Different Origins

The water-absorption rate of all four batches increased with immersion time, but the kinetic curves, uptake velocities and the times needed to reach a given absorption level differed markedly among provenances (Figure 1A-D). Two indicators, the instantaneous water-

Copyright @ STEMM Institute Press

absorption rate and the time to reach the 70 % threshold, were adopted for quantitative comparison [3,4]. Gansu samples exhibited the slowest kinetics overall (Figure 1A): the absorption rate was only 17.3 % at 30 min, remained below 20 % for a prolonged period and approached 70 % only after 360 min of immersion, without any saturation plateau within the observation window, indicating strong resistance to water penetration inside the tissue. The Yunnan batch showed moderately slow uptake (Figure 1D), exceeding 20 % at 20 min and reaching nearly 70 % at 90 min; it still belonged to the slow-absorbing group, with no obvious saturation inflection within the experimental timeframe.

Inner-Mongolia and Shanxi samples displayed rapid water-absorption characteristics (Figure 1B and C). The Inner-Mongolia batch reached 19.4 % at 5 min and approached 70 % at 30 min, with early-stage uptake markedly higher than that of the Gansu and Yunnan groups but lower than that of the Shanxi group. Among the four batches, the Shanxi-derived samples yielded the highest absorption rates (Figure 1C): 48.8 % at 5 min, above 70 % at 15 min and 86.9 % at 40 min, after which the curve slope decreased sharply and the trace levelled off, indicating that the Shanxi material approached a saturation state around 40 min. Such a plateau feature was absent in the other three origins within the observation window.

At 5 min, the absorption rates followed the order Shanxi (48.8 %) > Inner Mongolia (19.4 %) > Gansu (17.3 %) > Yunnan (< 20 %), whereas the times required to reach the 70 % threshold ranked as Shanxi (15 min) < Inner Mongolia (30 min) < Yunnan (90 min) < Gansu (360 min). All four groups obeyed a common pattern of fast initial uptake followed by progressive decay of the absorption rate. Given the presumably similar chemical compositions of the samples, the divergent kinetics imply region-specific differences in internal microstructure, which constitute the intrinsic factor underlying heterogeneous water-uptake properties [5,6].

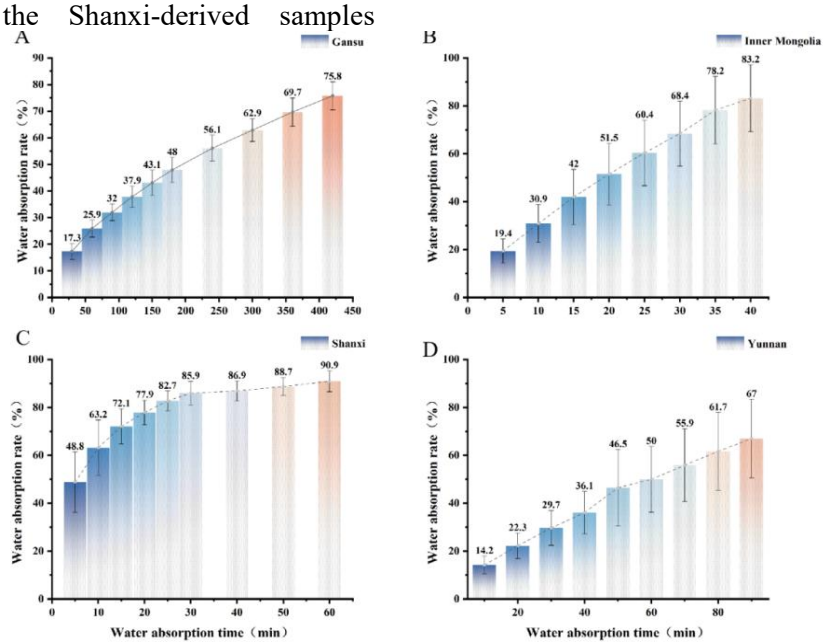


Figure 1. Water Absorption Rate Curves of Different Origins: (A) Gansu; (B) Inner Mongolia; (C) Shanxi; (D) Yunnan

3.2 Fitting Function of the Mass-Time Relationship

The mass-variation curves of the four batches during water uptake are shown in Figure 2. The datasets of the Gansu, Shanxi and Inner-Mongolia samples were fitted with the two-phase exponential decay (ExpDec2) model:

$$y=A_1\times e^{-\frac{x}{t_1}}+A_2\times e^{-\frac{x}{t_2}}+y_0 \quad (1)$$

The fitting parameters are summarised in Table 1. All three coefficients of determination exceeded 0.999, indicating excellent agreement between the experimental and model-predicted values. The two independent exponential terms correspond to distinguishable fast- and slow-uptake sub-processes, revealing that water ingress proceeds via two kinetically distinct stages (Figure 2).

In contrast, the mass-change curve of the

 Copyright @ STEMM Institute Press

Yunnan batch could not be satisfactorily characterised by the ExpDec2 function; instead, the two-phase exponential association (ExpAssoc) model provided a good fit:

$$y=A_1\times(1-e^{-\frac{x}{t_1}})+A_2\times(1-e^{-\frac{x}{t_2}})+y_0 \quad (2)$$

The corresponding parameters are listed in Table 1, with a coefficient of determination of approximately 0.999. The discrepancy in the optimal fitting functions reflects an intrinsic divergence in the mass-gain evolution patterns: the exponential-decay terms of ExpDec2 reproduce the mass-time trajectories of the Gansu, Shanxi and Inner-Mongolia groups, whereas the exponential-association terms of ExpAssoc reproduce the progressive mass accumulation of the Yunnan samples. Although all four groups exhibited increasing mass with immersion time, the mathematical form of their kinetic trajectories diverges, demonstrating that geographical provenance alters the fundamental mode of mass accumulation [7,8].

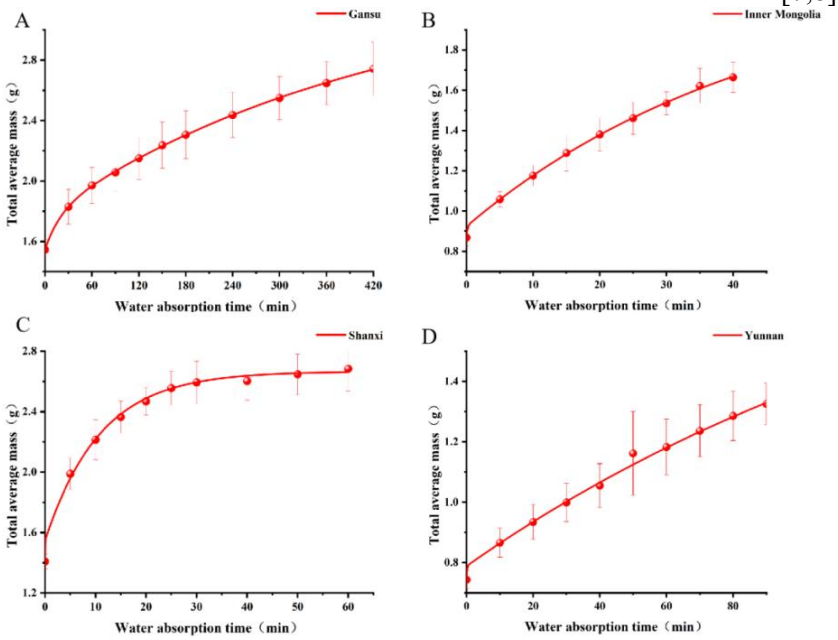


Figure 2. Water Absorption Mass Curves of Different Origins: (A) Gansu; (B) Inner Mongolia; (C) Shanxi; (D) Yunnan

Table 1. Fitting Parameters of Water Absorption Time-Total Average Mass Function

Origin	y_0	A_1	t_1	A_2	t_2	R^2(COD)
Gansu	3.30624	-0.22797	19.2244	-1.53293	423.72584	0.99992
Shanxi	2.66522	-0.13699	0.03332	-1.11982	10.85959	0.99911
Inner Mongolia	2.17708	-0.05538	0.13605	-1.25317	44.39081	0.99977
Yunnan	0.74353	0.04489	0.17172	1.29517	166.40869	0.99916

3.3 Water-State Evolution Revealed by T2 Inversion Spectra

The T2 inversion spectra of Astragalus membranaceus from the four origins exhibited three distinguishable peaks, namely T21 (0.01–1 ms), T22 (1–10 ms) and T23 (10–100 ms) (Figure 3). These peaks correspond to tightly bound water confined inside the herbal matrix (T21), semi-bound water generated through physical adsorption and chemical interactions (T22) and free water (T23), respectively. As water absorption proceeded, the overall moisture content and the uptake rate increased, accompanied by a continuous elevation of the magnetic-resonance peak amplitudes (Figure 3). Before immersion, water within the samples existed predominantly as tightly bound water, together with a fraction of semi-bound water and trace amounts of free water.

With prolonged immersion, the T2 spectral profile displayed a consistent rightward shift, with the transverse-relaxation time and signal amplitude increasing synchronously. This coupled variation directly indicates a progressive increase in the proportion of mobile water molecules within the herbal tissues [9,10]. The spectral shift and amplitude evolution reveal two co-occurring trends. First, water molecules continuously migrate into the internal matrix, raising the total water content and increasing the peak signal intensity. Second,

Copyright @ STEMM Institute Press

newly ingested water alters the micro-environmental confinement of the original water-binding sites, which prolongs the transverse-relaxation time and accounts for the rightward shift of the spectral curves. The coexistence of three resolved peaks throughout immersion shows that multiple water populations with distinct mobilities coexist within the samples, corroborating the macroscopic water-absorption kinetics described above [11].

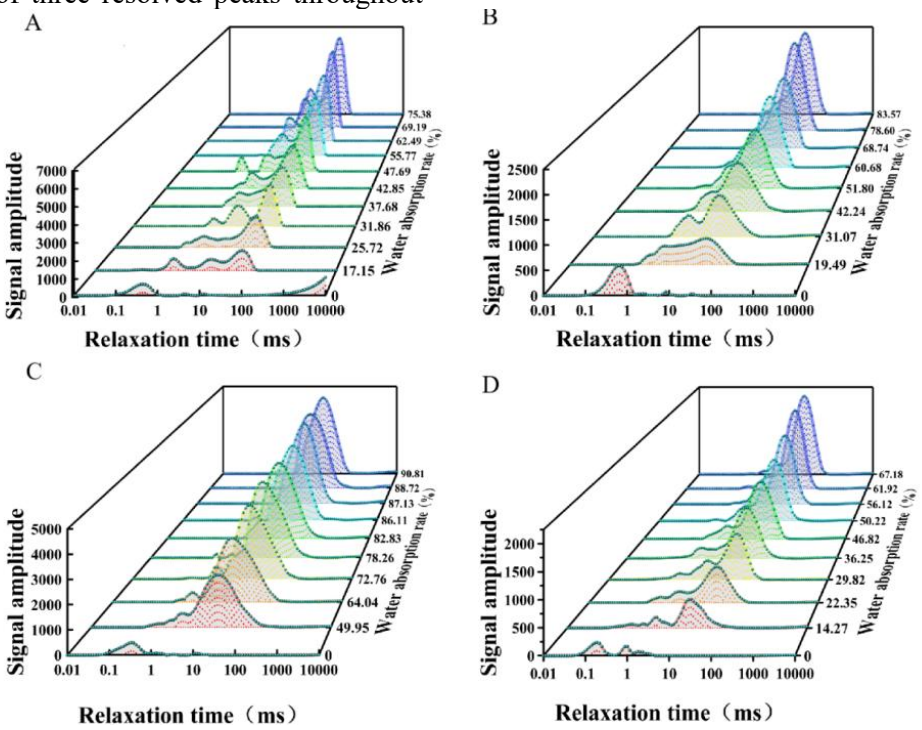


Figure 3. Inverse Curve of Transverse Relaxation during the Water Absorption Process of Astragalus from Different Origins: (A) Gansu; (B) Inner Mongolia; (C) Shanxi; (D) Yunnan

3.4 Linear Correlation between Absorbed Mass and NMR Signal

The transverse-relaxation magnetic-resonance signal is expressed as Eq. (3), where the signal intensity M is proportional to the hydrogen-proton density ρH, which is positively correlated with the sample water content. In the inversion spectra, the total peak area quantifies the overall magnitude of the magnetic-resonance signals. Figure 4 illustrates the relationship between the average total mass and the total integrated peak area of the four batches throughout water absorption.

$$M=k\rho_H e^{-\frac{t}{T_2}} \quad (3)$$

Robust linear correlations between the average total mass and the average total peak area were obtained for all four origins (Figure 4). The derived linear regression functions and the corresponding coefficients of determination are listed below:

Gansu:

$$y=-70167.16781+50011.24803x \quad (4)$$

Shanxi:

$$y=-59092.30669+45736.07481x \quad (5)$$

Inner Mongolia:

$$y=-30517.77926+42104.05564x \quad (6)$$

Yunnan:

$$y=-33624.31243+49298.06451x \quad (7)$$

All four datasets yielded R^2 values exceeding 0.99, confirming a strong linear coupling between mass gain and NMR signal enhancement during water uptake. The regression parameters differed across provenances in both slope and intercept: the slope reflects the NMR signal increment per unit mass gain, while the intercept represents the baseline signal offset. The Shanxi samples achieved the highest R^2 (0.99893), indicating the tightest mass-signal correspondence, whereas the Yunnan group exhibited the lowest R^2 (0.99313) while still showing excellent linearity. Such consistently high R^2 values [9,10] cross-validate that the increase in absorbed water mass is directly reflected by the elevation of the total peak area in the inversion spectra. Although the four origins differed markedly in macroscopic absorption rates and microscopic water-phase distributions, the linear

 Copyright @ STEMM Institute Press

linkage between gravimetric mass change and LF-NMR signal response persisted across all batches. Accordingly, magnetic-resonance signals can serve as a reliable proxy for characterising the water-absorption behaviour of Astragalus membranaceus, bridging macroscopic gravimetric measurement and microscopic transverse-relaxation characterisation.

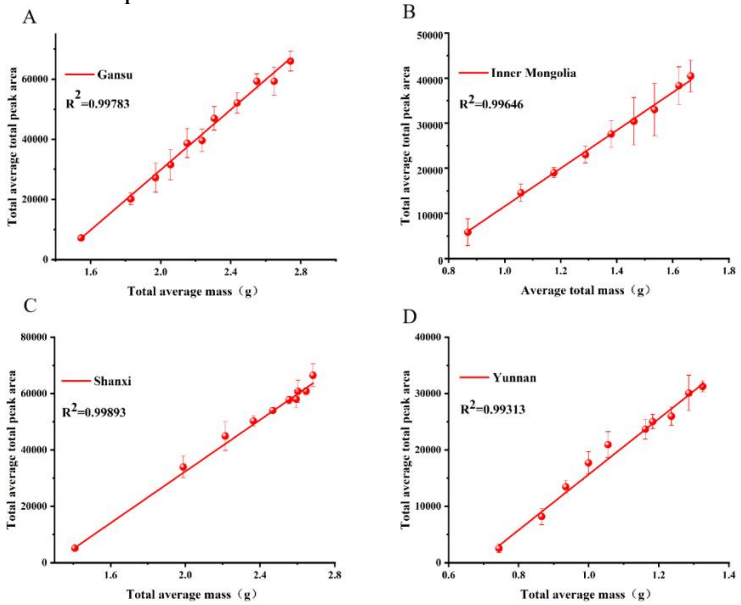


Figure 4. Diagram of the Relationship between Water Absorption Mass and Transverse Relaxation Signal from Different Origins: (A) Gansu; (B) Inner Mongolia; (C) Shanxi; (D) Yunnan

4. Discussion

4.1 Principal Results

This study quantified the water-uptake behaviour of Astragalus membranaceus from four major producing regions by LF-NMR transverse-relaxation measurements with the CPMG pulse sequence, aiming to establish a non-destructive characterisation tool for this medicinal herb. Pronounced inter-provenance discrepancies were observed in the absorption kinetics, which are attributed to region-specific internal microstructural differences rather than to bulk chemical composition. The Shanxi-sourced samples absorbed water most quickly, reaching the 70 % threshold at 15 min and approaching saturation at about 40 min; by contrast, the Gansu samples required 360 min to reach 70 % absorption and never reached saturation within the observation window. The T2 inversion spectra resolved three water fractions, and the free-water fraction increased progressively while the bound-water content remained nearly constant, accompanied by synchronous elevation and rightward shift of the spectral signals. Gravimetric total mass exhibited strong positive linear correlations with the LF-NMR total peak area across all four provenances, with all coefficients of determination above 0.99, validating that LF-NMR signals can serve as a reliable non-invasive proxy for monitoring water-uptake dynamics.

4.2 Limitations

This study has several limitations. First, the sample set covered only four representative geographical origins; cultivar, harvest-year, cultivation-mode and storage-condition variants were not included in the present analysis [3], so the generalisability of the observed kinetic patterns to broader sample cohorts remains to be tested. Second, the interpretation relies mainly on microstructural water-transport behaviour without direct compositional information; samples with highly similar microstructures might exhibit comparable absorption profiles. Third, all experiments were conducted under strictly controlled laboratory conditions, and on-site industrial fluctuations in temperature, humidity and sample surface status may interfere with the relaxation measurements. Future work should expand the sample library, combine NMR data with compositional fingerprints and perform pilot-scale validation

Copyright @ STEMM Institute Press

under realistic conditions [4].

4.3 Comparison with Prior Work

Most existing LF-NMR studies of hygroscopic biological materials have focused on static water-state characterisation of raw or processed samples [9,10]. In contrast, the present work collected dynamic time-series transverse-relaxation signals throughout the whole water-absorption procedure, allowing the kinetic mode of water ingress to be quantified through mass-time fitting functions and linear mass-signal correlations. Compared with conventional chromatographic and spectroscopic protocols that demand destructive pre-treatment, the LF-NMR route avoids chemical reagents and provides rapid, repeatable measurements on intact herbal tissues. Nevertheless, because the relaxation response originates from water protons rather than from specific secondary metabolites, the workflow yields no direct chemical information and is accordingly positioned as a complementary screening layer; positive hits can subsequently be verified with compositional assays [4,5].

5. Conclusion

This study characterised water-absorption kinetics and water-state dynamics of Astragalus membranaceus from Gansu, Inner Mongolia, Shanxi and Yunnan using an LF-NMR-based approach. Significant inter-provenance differences were observed in the absorption rate, the saturation-onset time and the mathematical mode of mass accumulation, reflecting intrinsic variations in internal tissue microstructure. The T2 spectral analysis demonstrated consistent variation patterns of bound and free water during water infiltration, and the excellent linear correlation between gravimetric mass change and LF-NMR signal intensity ($R^2 > 0.99$) enables non-invasive tracking of the water-uptake process. The two-phase exponential decay and association functions concisely describe the mass-time trajectories, and the mass-signal linear relationships provide a quantitative basis for monitoring moisture behaviour in porous medicinal matrices. Compared with conventional chemical assays, the present method bypasses complex sample pre-processing and offers a reference technique for rapid physical quality assessment of Astragalus membranaceus and other porous-matrix medicinal herbs.

Acknowledgments

This work was financially supported by Entrepreneurship and Innovation project of Hainan Medical University (S202411810012), Ministry of Education's Cooperative Education Project (NO.241201416190522, NO.250601416251501), Academic Enhancement Support Program of Hainan Medical University (XSTS2026180) and Hainan Medical University's research start-up fund.

References

[1] Gu X.P., Yang L.L., Dong C.M., et al. Research progress on the formation mechanism and regulation of the quality of traditional Chinese medicinal materials. Northern Horticulture, 2024, (06): 129-137.

[2] Jia B.T., Liu H.C., Wang Y.Y., et al. Improving the quality of traditional Chinese medicinal materials and focusing on clinical evidence-based practice in traditional Chinese medicine: insights from Academician Zhang Boli on the key to high-quality development of traditional Chinese medicine. Chinese Journal of Integrated Traditional and Western Medicine, 2023, 43(1): 21-23.

[3] Shao J.M., Lian Y.F., Yan L.H., et al. Comparative analysis of total saponins in Astragalus from different producing areas. Shaanxi Journal of Traditional Chinese Medicine, 2018, 39(2): 268-270.

[4] Ozel B., Oztop M.H. A quick look to the use of time domain nuclear magnetic resonance relaxometry and magnetic resonance imaging for food quality applications. Current Opinion in Food Science, 2021, 41: 122-129.

[5] Hou X.W., Wang G.L., Su G.Q., et al. Rapid identification of edible oil species using supervised support vector machine based on low-field nuclear magnetic resonance relaxation features. Food Chemistry, 2019, 280: 139-145.

[6] Lankhorst P., Chang A.N. The application of NMR in compositional and quantitative analysis of oils and lipids.Modern Magnetic Resonance. Cham: Springer, 2017: 1-22.

[7] Jiang X.M., Yang D.H., Xiang G.Q., et al. Determination of cis/trans fatty acid contents in edible oils by 1H NMR spectroscopy in association with multivariate calibration. Journal of Food

 Copyright @ STEMM Institute Press

Composition and Analysis, 2022, 105: 104195.

[8] Liu Y., Sun L.J., Du C.S., et al. Near-infrared prediction of edible oil frying times based on Bayesian ridge regression. Optik, 2020, 218: 164950.

[9] Duan S.F., Chen Y., Xu W.E., et al. Study on the moisture change law during maize kernel development based on low-field nuclear magnetic resonance technology. Journal of Maize Sciences, 2024, 32(2): 69-76.

[10]Zhang Y., Zhao Y.N., Zhao J.X., et al. Detection and discrimination of soybean oil content based on low-field nuclear magnetic resonance technology with various dimensions. Transactions of the Chinese Society of Agricultural Engineering, 2024, 40(4): 337-344.

[11]Ren L.H., Wang F.C., Zhang Y.L., et al. Rapid identification of Radix Astragali by data fusion of laser-induced breakdown spectroscopy and Raman spectroscopy coupled with deep learning. Talanta, 2025, 282: 127016.

Copyright @ STEMM Institute Press